JOURNAL OF VIROLOGY, Feb. 2010, p. 1816–1827 Vol. 84, No. 4
0022-538X/10/$12.00 doi:10.1128/JVI.01665-09
Copyright © 2010, American Society for Microbiology. All Rights Reserved.

Intergenotypic Replacement of Lyssavirus Matrix Proteins Demonstrates the Role of Lyssavirus M Proteins in Intracellular Virus Accumulation▽

Stefan Finke,[1]* Harald Granzow,[2] Jose Hurst,[1]† Reiko Pollin,[1] and Thomas C. Mettenleiter[1]

Friedrich-Loeffler-Institut, Federal Research Institute for Animal Health, Institutes of Molecular Biology[1] and Infectology,[2] D-17493 Greifswald–Insel Riems, Germany

Received 8 August 2009/Accepted 21 November 2009

Lyssavirus assembly depends on the matrix protein (M). We compared lyssavirus M proteins from different genotypes for their ability to support assembly and egress of genotype 1 rabies virus (RABV). Transcomplementation of M-deficient RABV with M from European bat lyssavirus (EBLV) types 1 and 2 reduced the release of infectious virus. Stable introduction of the heterogenotypic M proteins into RABV led to chimeric viruses with reduced virus release and intracellular accumulation of virus genomes. Although the chimeras indicated genotype-specific evolution of M, rapid selection of a compensatory mutant suggested conserved mechanisms of lyssavirus assembly and the requirement for only few adaptive mutations to fit the heterogenotypic M to a RABV backbone. Whereas the compensatory mutant replicated to similar infectious titers as RABV M-expressing virus, ultrastructural analysis revealed that both nonadapted EBLV M chimeras and the compensatory mutant differed from RABV M expressing viruses in the lack of intracellular viruslike structures that are enveloped and accumulate in cisterna of the degranulated and dilated rough endoplasmic reticulum compartment. Moreover, all viruses were able to bud at the plasma membrane. Since the lack of the intracellular viruslike structures correlated with the type of M protein but not with the efficiency of virus release, we hypothesize that the M proteins of EBLV-1 and RABV differ in their target membranes for virus assembly. Although the biological function of intracellular assembly and accumulation of viruslike structures in the endoplasmic reticulum remain unclear, the observed differences could contribute to diverse host tropism or pathogenicity.

Downloaded from jvi.asm.org at FRIEDRICH-LOEFFLER-INSTITUT on February 9, 2010

Rabies virus (RABV) and rabies-related rhabdoviruses are classified to the lyssavirus genus (13). Among the lyssaviruses various genotypes have evolved with differences in host species tropism and pathogenicity. For instance, members of genotype 1 rabies viruses circulate in terrestrial mammals and in bats, whereas members of other genotypes, such as genotypes 5 and 6 (European bat lyssavirus types 1 and 2 [EBLV-1 and ELBV-2]), are mainly restricted to bats. Although EBLVs appear adapted to their bat reservoir hosts, they have retained the ability to infect terrestrial mammals including humans, as indicated by occasional infection of humans and terrestrial animals such as sheep, stone marten, or cats (9, 35, 42). These are typically dead end infections with no further spread in the new host species. Experimental infection of sheep indicated that EBLVs are less pathogenic than genotype 1 viruses in the heterologous host (1, 7, 46, 47).

Although the replication potentials of various lyssaviruses appear different in a given host, the genome organization is highly conserved (11, 27), containing only five virus genes that are sequentially ordered as individual cistrons. Whereas the viral nucleoprotein N, phosphoprotein P, and large polymerase L are essential for RNA synthesis (8), the envelope components matrix protein M and glycoprotein G are required for virus release and virus infectivity, respectively (31, 32).

Based on receptor binding and the apoptosis-inducing properties of the sole RABV surface antigen G, G protein has been designated as the major pathogenicity determinant of genotype 1 lyssaviruses (15, 33, 34). However, several examples for G-independent mechanisms of virus-cell interaction exist (2, 3, 6, 30, 41, 44, 45), some of which have been shown to be involved in escape from antiviral innate immune responses and to be important for virus replication *in vivo*.

One viral protein that has been noticed as an important RABV pathogenicity determinant is the matrix protein M (12, 39). M is essential for virus assembly and release (32) and is able to support virus budding even in the absence of G (31). In addition, RABV M regulates viral RNA synthesis (14, 17) and has been described to contribute to TRAIL-dependent induction of apoptosis (25) and to mitochondrial dysfunction (18). Recently, the X-ray crystal structure analysis of M of genotype 2 Lagos bat lyssavirus demonstrated a high conservation of M structures within the rhabdovirus family, despite the lack of sequence conservation between the lyssavirus and vesiculovirus genera (19).

With 92.3% identity, the amino acid sequences of lyssavirus M proteins are highly conserved within the lyssavirus genus (11) but also contain differences that either may reflect intragenotypic coevolution with other virus proteins or divergence caused by different host adaptation and/or pathogenicity. To

* Corresponding author. Mailing address: Friedrich-Loeffler-Institut, Südufer 10, D-17493 Greifswald-Insel Riems, Germany. Phone: 49 38351 7243. Fax: 49 38351 7275. E-mail: stefan.finke@fli.bund.de.

† Present address: Sektion Experimentelle Virologie, Universitätsklinikum Tübingen, Elfriede-Aulhorn-Strasse 6, 72076 Tübingen, Germany.

▽ Published ahead of print on 2 December 2009.

analyze the compatibility of M proteins from bat lyssaviruses in a rabies virus genetic background, we tested the ability of EBLV M proteins to support RABV replication after transient complementation and in chimeric viruses. Replacement of RABV M with EBLV-1 M resulted in a strong decrease in infectious virus production, suggesting the presence of a rather high degree of genotype-specific constraints. Surprisingly, recovery of efficiently replicating virus was achieved after only three passages, indicating that minor changes in M or M-interacting proteins may restore full budding activity in the genotype 1 context. Moreover, none of the chimeric viruses, neither the inefficiently released chimeric viruses nor the efficiently released passaged mutant, was able to support intracytoplasmic budding of viruslike structures at membranes of the rough endoplasmic reticulum (rER). Intracellular accumulation of enveloped viruslike structures in the rER is a common phenomenon of several rabies and rabies-related viruses (36, 37) that was obviously lost in the chimeric viruses. The lack of intracellular virus assembly strongly suggests that EBLV-1 and RABV M differ in their cellular target membranes for virus assembly and budding.

MATERIALS AND METHODS

Cells and viruses. BSR T7/5 cells (4) and the production of NPgrL virus with the M and G gene deleted on a MGon packaging cell line (17) were performed as described previously.

Recombinant virus rescue. Recombinant RABVs were rescued by cotransfection of full-length genome cDNA and expression plasmids into BSR T7/5 cells as described previously (16). In contrast to the previous protocol, expression of the full-length genomic RNA was driven by the human cytomegalovirus immediate-early promoter (CMVie) in the full-length cDNA plasmid pCMV-SADL16. The RABV N, P, and L proteins were expressed in an RNA-polymerase II-dependent manner from the cotransfected plasmids pCAGGS-N, pCAGGS-P, and pCAGGS-L.

cDNA construction. For the establishment of a T7-RNA polymerase independent rescue system, the previously described full-length cDNA clone pSAD L16 (40) was modified by insertion of a CMVie promoter/enhancer sequence from pcDNA3.1neo (Invitrogen) upstream of the cloned virus cDNA. To allow the synthesis of a correct 5′ terminus of the transcribed full-length antigenome RNA, a synthetic hammer head ribozyme sequence that was previously used for the rescue of lyssavirus minigenomes (26) was inserted between the CMVie and the viral cDNA sequences, resulting in the full-length cDNA clone pCMV-SADL16. Expression plasmids for the RABV N, P and L proteins were generated by PCR amplification of the coding sequences (CDs) from the full-length clone pSAD-L16 (40) and insertion into the plasmid vector pCAGGS (38).

For transient expression of RABV and EBLV-1 M proteins, the M CDs were PCR amplified from pCMV-SAD L16 and cloned cDNAs of EBLV-1 strain RV9 and EBLV-2 (for sequences, see reference 27) and inserted into expression plasmid pCAGGS (38). For the construction of the chimeric pSAD EBLV-1 M and pSAD EBLV-2 M, NheI and NotI restriction sites were introduced into the 5′ and 3′ noncoding sequences of the M gene of pCMV-SAD L16, and PCR-amplified EBLV-1 M, and EBLV-2 M CDs were introduced. The EBLV-1 M amino acid sequence was identical to a previously published EBLV-1 M sequence (Swiss-Prot accession no. A4UHQ0) except for one amino acid at position 47 (K47R). The EBLV-2 M protein differed from a previously published EBLV-2 M sequence (GenBank accession no. ABZ81189) at two amino acid positions (A100D and S153L). As a control, RABV M was reintroduced with the same strategy, resulting in pSAD RABV M.

Transcomplementation of NPgrL virus. A total of 10^6 BSR T7/5 cells were infected with NPgrL at a multiplicity of infection (MOI) of 1. Two days after infection 5 μg of pCAGGS RABV M, pCAGGS EBLV-1 M, or pCAGGS EBLV-2 M and 5 μg of pCAGGS RABV G were cotransfected by using polyethyleneimine transfection reagent (Sigma-Aldrich) at 1 μg/μl in H_2O. At 48 h after DNA transfection, 2 ml of cell culture supernatant was harvested and cleared from the cell debris by centrifugation (5 min, 6,000 × *g*, 4°C). Then, 1 ml was transferred onto 10^6 BSR T7/5 cells, and green fluorescent protein (GFP) expression from NPgrL virus was detected by fluorescence microscopy after 48 h of incubation. The remaining supernatant was used for infectious virus titration by endpoint dilution.

Indirect immunofluorescence microscopy. For indirect immunofluorescence, the monolayer cultures were fixed with 3% paraformaldehyde and permeabilized with 0.5% Triton X-100 in phosphate-buffered saline (PBS). Virus-infected cells were detected using a monospecific polyclonal rabbit anti-P serum (P160/5; diluted 1:2,000 in PBS) and anti-rabbit Alexa Fluor 488 conjugate (Molecular Probes) at 1:1,000 in PBS on a Keyence BZ-8000 microscope. The sizes of the foci were established by using ImageJ software.

RNA analysis. RNA was prepared with an RNeasy minikit (Qiagen) according to the supplier's instructions. For the preparation of virion RNA, supernatants from 9×10^6 BSR T7/5 cells were pelleted through a 5-ml 20% sucrose cushion in TEN buffer (50 mM Tris-HCl [pH 7.4], 1.0 mM EDTA, 150 mM NaCl [pH 7.4]) by ultracentrifugation (SW32, 32,000 rpm, 4°C, 2 h) prior to RNA isolation. The isolated RNAs were separated in 1% formaldehyde gels and blotted on positively charged nylon membranes (Hybond-N+; GE Healthcare). For the detection of virus RNAs, the 1.3-kb N CDs were PCR amplified from pCAGGS-RVN and labeled with [α-^{32}P]dCTP by using the nick translation system (Invitrogen).

Electron microscopy. For electron miscroscopy analysis, BSR T7/5 monolayer cells were infected at an MOI of 3 and fixed at 46 h postinfection (p.i.) for 60 min with 2.5% glutaraldehyde buffered in 0.1 M sodium cacodylate (pH 7.2; 300 mosmoles; Merck, Darmstadt, Germany). They were then scraped off the plate, pelleted by low-speed centrifugation, and embedded in LMP agarose (Biozym, Oldendorf, Germany). Small pieces were cut with a razor blade, postfixed in 1.0% aqueous OsO_4 (Polysciences Europe, Eppelheim, Germany), and stained with uranyl acetate. After stepwise dehydration in ethanol, the cells were cleared in propylene oxide, embedded in Glycid Ether 100 (Serva, Heidelberg, Germany), and polymerized at 59°C for 4 days.

Ultrathin sections of embedded material, counterstained with uranyl acetate and lead salts, were examined with an electron microscope (Philips Tecnai 12; Philips, Eindhoven, The Netherlands).

RESULTS

EBLV M complements M-deficient RABV. In order to test the ability of lyssavirus genotype 5 and 6 M protein to complement M-deficient genotype 1 RABV, cells infected by NPgrL virus with the M and G gene deleted were transfected with expression plasmids for RABV G and different M proteins. At 2 days after transfection, cell culture supernatants were harvested, and the presence of infectious NPgrL virus was assessed by infection of BSR T7/5 cells. NPgrL-derived GFP expression was detected by fluorescence microscopy after further 2 days of infection (data not shown). Both EBLV-1 M and EBLV-2 M were able to support the release of infectious NPgrL virus, whereas in the absence of M, no infectious virus was detectable in the cell culture supernatants. The levels of infectious virus, however, were strongly decreased for EBLV-1 M and EBLV-2 M compared to the authentic RABV M, which led to the infection of almost 100% of the cells. Determination of the infectious virus titers in the cell culture supernatants showed that release of infectious virus was 10- and 100-fold decreased for EBLV-1 M and EBLV-2 M, respectively (Fig. 1A). Comparable synthesis of the different M proteins in the complementation experiments was controlled by Western blots with a cross-reactive serum raised against purified EBLV-2 M protein (Fig. 1B). Whereas for EBLV-2 M and RABV M nearly identical signals were obtained, an even stronger signal for EBLV-1 M strongly indicated that a low level expression of EBLV-1 M was not causative for the 10-fold decreased infectious virus titers for EBLV-1 M. The complementation data showed that the EBLV-1 and -2 M proteins exhibit a basal activity to produce infectious virus even in the genotype 1 RABV context. The efficiencies of infectious virus production, however, were strongly decreased.

Downloaded from jvi.asm.org at FRIEDRICH-LOEFFLER-INSTITUT on February 9, 2010

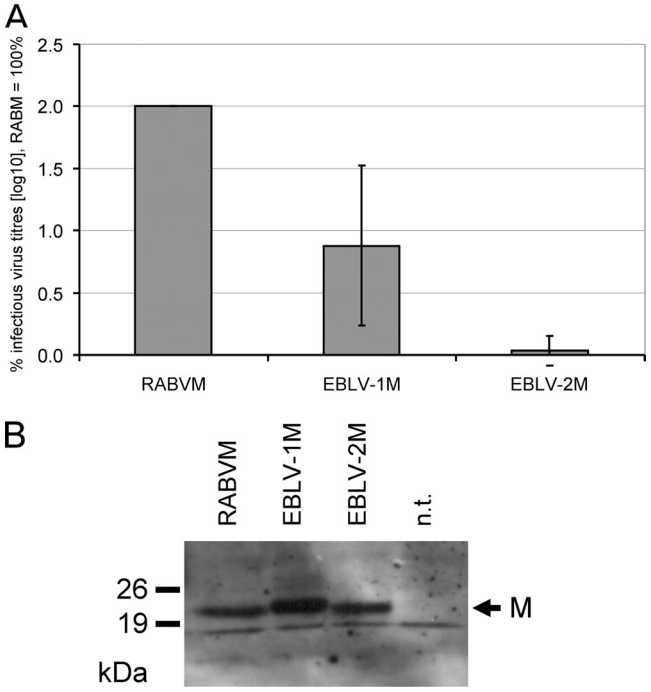

FIG. 1. Transcomplementation of genotype 1 RABV with EBLV-1 and EBLV-2 M. (A) NPgrL virus with the M and G genes deleted was complemented by coexpression of the indicated M proteins and RABV G from transfected plasmids. Two days after transfection, the infectious virus titers in the cell culture supernatants from the complementation experiments were determined by end point dilutions. An ~10-fold and ~100-fold decrease in the titers was observed for EBLV-1 M and EBLV-2 M, respectively ($n = 3$). (B) To control the expression of the different lyssavirus M proteins, cell extracts from a representative complementation experiment were analyzed in Western blots with an EBLV-2 M-specific serum. A background signal beneath M that was also present in not transfected (n.t.) cells was used as a loading control. Note that the serum is cross-reactive for all three M proteins. Due to expectable variations in the avidities to the heterologous EBLV-1 M and RABV M proteins, an exact quantitative comparison is not possible.

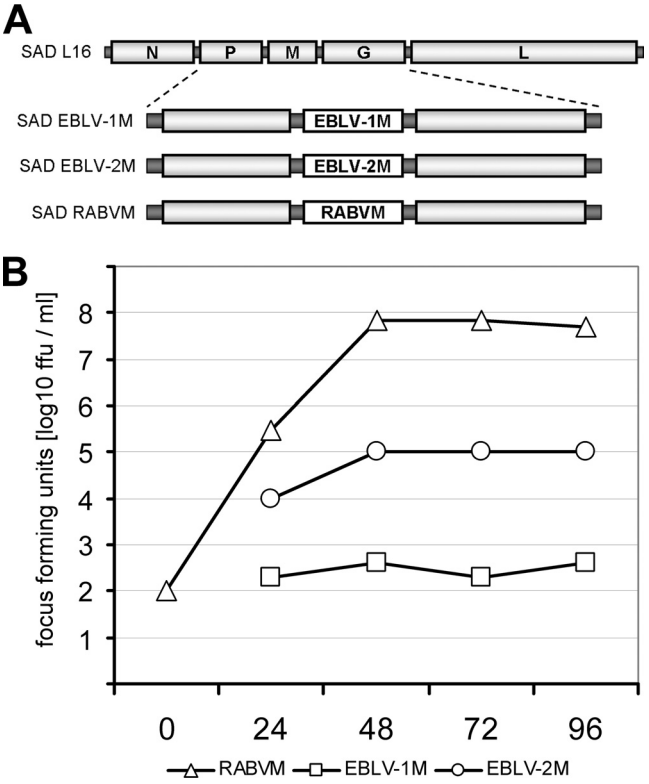

FIG. 2. Organization and growth kinetics of M chimeras. (A) The SAD L16 genome sequence was modified by replacement of the authentic M CDs with sequences for EBLV-1 M and EBLV2 M, resulting in SAD EBLV-1 M and SAD EBLV-2 M. Reinsertion of the authentic RABV M sequence led to SAD RABV M. All three recombinant genomes had identical 5′- and 3′-noncoding sequences within the M gene. (B) Multiple-step growth curves showed that SAD EBLV-1 M was strongly decreased in infectious virus production. From 48 to 96 h p.i., virus titers remained 5 logs below SAD RABV M titers. With end titers of 10^5, the titers for SAD EBLV-2 M were higher than those of SAD EBLV-1 M but remained 3 logs below the SAD RABV M titers. Note that the SAD EBLV-1 M and SAD EBLV-2 M stocks were directly taken from the transfected cell cultures of the rescue experiment in order to minimize adaptive mutations within the heterogenotypic M genes.

Rescue of chimeric viruses. To test whether EBLV-1 M and EBLV-2 M were able to mediate autonomous RABV replication, chimeric cDNAs pSAD EBLV-1 M and pSAD EBLV-2 M were constructed (Fig. 2A). In the chimeric cDNAs, the authentic RABV M CD has been replaced by the EBLV M open reading frames (ORFs). In addition, control cDNA pSAD RABV M was constructed with identical noncoding M gene sequences. From all three recombinant cDNAs, infectious viruses could be rescued, and the identities of the recombinant viruses were controlled by reverse transcription-PCR (RT-PCR) sequencing (data not shown). In contrast to standard rescue procedures for RABV (16), rescue of SAD EBLV-1 M and of SAD EBLV-2 M required multiple passages of the transfected cells until ~90% of the cells were infected and sufficient levels of virus for subsequent infections were detectable in the cell culture supernatants.

To determine the differences in virus spread after insertion of the EBLV M proteins into the genotype 1 genome backbone, SAD EBLV-1 M and SAD EBLV-2 M were used to infect BSR T7/5 monolayer cell cultures. After 36 h of infection, the foci of infected cells were detected by immunofluorescence, and their sizes were compared to SAD RABV M (not shown). The spread of SAD RABV M was readily detectable. Foci of SAD EBLV-2 M-infected cells were also visible, although they were smaller than those of SAD RABV M at this time after infection. Surprisingly, SAD EBLV-1 M was almost completely unable to spread, indicating that virus spread was heavily impaired in SAD EBLV-1 M. Accordingly, multiple-step growth curves after infection of BSR T7/5 cell cultures at an MOI of 0.001 showed that SAD EBLV-1 M was strongly decreased in infectious virus production (Fig. 2B). From 48 h p.i., the SAD EBLV-1 M titers were ~10^5-fold lower than SAD RABV M titers. The titers of SAD EBLV-2 M were ~10^3-fold lower than that those of SAD RABV M, indicating that EBLV-2 M complemented RABV better than EBLV-1 M.

Increased full-length genome accumulation in SAD EBLV-1 M- and SAD EBLV-2 M-infected cells. Viral RNA replication occurs rather inefficient in the absence of the regulatory M protein (17). Thus, decreased titers of chimeric viruses could

Downloaded from jvi.asm.org at FRIEDRICH-LOEFFLER-INSTITUT on February 9, 2010

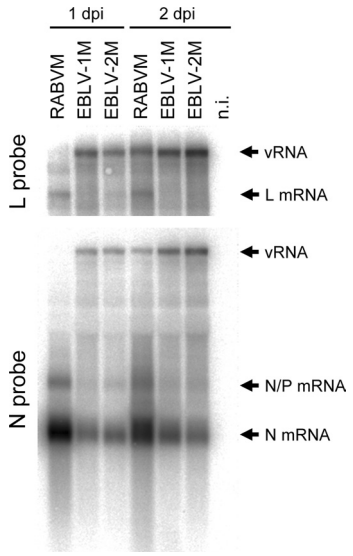

FIG. 3. Intracellular vRNA accumulation in SAD EBLV-1 M- and SAD EBLV-2 M-infected cells. Virus RNA accumulation in infected cells was monitored 1 and 2 days p.i. in Northern hybridizations with N- and L-gene specific cDNA probes. Abundant vRNA signals were detectable for SAD EBLV-1 M and SAD EBLV-2 M. Compared to SAD RABV M, the signal intensities were increased at both time points, whereas the levels of N and L mRNAs were lower. The hybridization signals obtained for N at 2 days p.i. were quantitated in a phosphorimager, and the ratios of genomic full-length RNA (vRNA) and monocistronic N mRNA signals were calculated. In SAD EBLV-1 M- and SAD EBLV-2 M-infected cells the N mRNA/vRNA ratios were 17- and 42-fold decreased, respectively, compared to SAD RABV M.

reflect limiting levels of replication products caused by low or absent stimulatory effects of the hetero-genotypic M proteins on the viral RNA synthesis machinery. To analyze the intracellular level of full-length virus RNA (vRNA), BSR T7/5 cells were infected with SAD EBLV-1 M, SAD EBLV-2 M, and SAD RABV M at an MOI of 1. Since limited amounts of virus containing supernatant directly from transfected cells made high-MOI infections impossible, for these experiments virus stock from the first supernatant passage was used. At 1 and 2 days p.i., RNA was prepared from the infected cells, and viral RNA accumulation was monitored by Northern hybridizations with N- and L-gene-specific cDNA probes (Fig. 3). Whereas in SAD RABV M-infected cells the highest N mRNA levels were detected, genome accumulation of SAD RABV M was lower than in SAD EBLV-1 M- and SAD EBLV-2 M-infected cells. Thus, higher full-length RNA levels were present in cells infected with the chimeric viruses. Limited full-length RNA levels could therefore be excluded as the cause of the observed decrease in infectious virus production.

The Northern blot signals for N mRNA and full-length vRNA after 2 days of infection were quantitated by phosphorimaging, and the ratios of N mRNA/vRNA were calculated. Compared to control virus SAD RABV M, in SAD EBLV-1 M- and SAD EBLV-2 M-infected cells, the mRNA/vRNA ratios were 17- and 42-fold decreased, either suggesting increased stimulatory activities of the heterogenotypic M proteins on virus RNA replication or the accumulation of replication products as a consequence of inefficient virus release.

Intracellular accumulation of viruslike structures in SAD RABV M- but not in SAD EBLV-1 M- and SAD EBLV-2 M-infected cells. To assess whether the loss of function by the heterogenotypic M proteins correlated with intracellular accumulation of condensed RNP, infected BSR T7/5 cells (MOI = 3) were analyzed by electron microscopy after 2 days of infection. Analysis of cells infected with RABV strain SAD L16 showed budding processes at different cellular membranes, and intracellular accumulation of viruslike structures in dilated and degranulated cisterna of the rER (Fig. 4A). Cross-sections

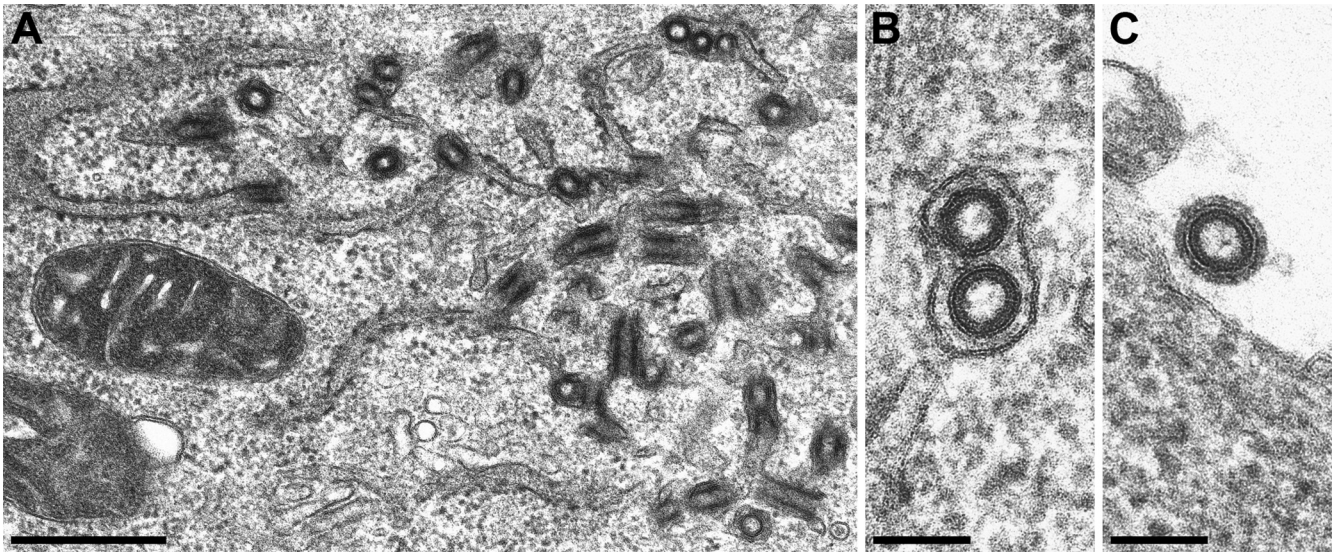

FIG. 4. Accumulation of viruslike structures in the rER of RABV-infected cells. Electron microscopic analysis of SAD L16-infected BSR T7/5 monolayer cell cultures was performed. (A) Viruslike structures accumulated in the dilated and degranulated rER of infected cells. Scale bar, 500 nm. (B) Cross-sections of viruslike structures in degranulated rER cisterna. Scale bar, 100 nm. (C) Cross-section of an extracellular virus particle. Scale bar, 100 nm.

Downloaded from jvi.asm.org at FRIEDRICH-LOEFFLER-INSTITUT on February 9, 2010

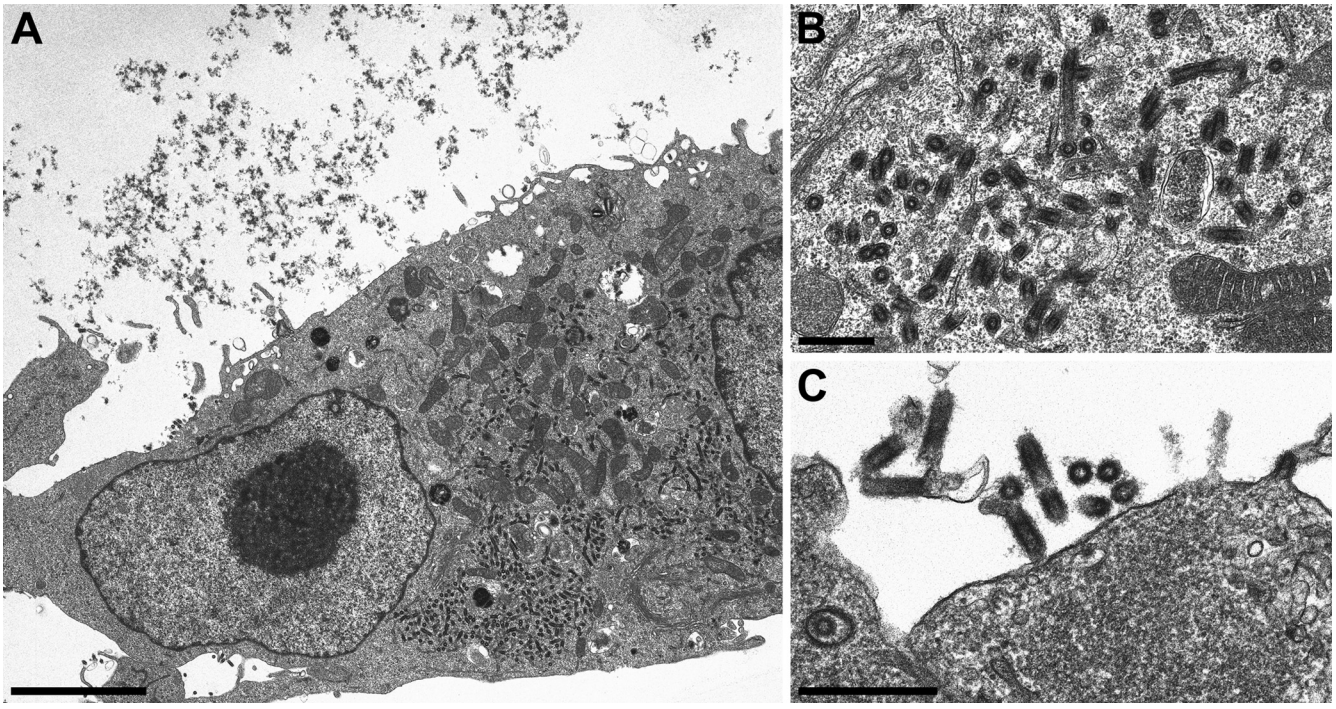

FIG. 5. Accumulation of intracellular viruslike structures in SAD RABV M-infected cells is comparable to the authentic SAD L16 virus. Electron microscopic analysis of SAD RABV M-infected BSR T7/5 monolayer cell cultures. (A) Intracellular viruslike structures. Scale bar, 4 μm. (B) Higher magnification of intracisternal structures indicate accumulation in the rER. Scale bar, 500 nm. (C) Extracellular virions derived from budding at the plasma membrane. Scale bar, 500 nm.

of intracisternal viruslike structures revealed an envelope (Fig. 4B). Comparison with extracellular virus particles revealed that the intracisternal viruslike structures were identically organized with respect to the inner architecture and particle diameter. A distinct layer of densely arranged glycoprotein projections on the surface, however, was only detectable on extracellular virions (Fig. 4C). This raises the question whether the intracisternal viruslike structures contain viral glycoprotein in the same amount and arrangement as mature extracellular virions.

Recombinant SAD RABV M revealed the same phenotype as SAD L16 with strong accumulation of intracisternal viruslike structures in the dilated and degranulated rER compartment, showing that the alterations in the noncoding sequences of the M genes did not lead to detectable alterations in virus assembly (Fig. 5).

In striking contrast, infections with SAD EBLV-1 M or SAD EBLV-2 M showed a different phenotype. Infection with either SAD EBLV-1 M or SAD EBLV-2 M did not lead to the accumulation of viruslike structures in the rER (Fig. 6 and 7). Moreover, no accumulations of condensed RNPs in the cytoplasm or beneath cellular membranes were detectable, indicating that inefficient production of infectious virus was not a result of defects in late assembly steps but more likely was attributable to failure of RNP recruitment by M protein. In contrast to the lack of intracellular viruslike accumulations, virus budding at the cell membrane was detectable (Fig. 6B), showing that RNP-condensation and particle release also occurred in SAD EBLV-1 M- and SAD EBLV-2 M-infected cells.

The observed differences in intracellular viruslike accumulations between SAD RABV M- and the ELBV M-expressing viruses were verified in Vero cells and cell lines derived from *Eptesicus serotinus* bats, the main natural reservoir of EBLVs (results not shown).

Successive passages of SAD EBLV-1 M result in increased infectious virus titers. The observed intracellular accumulation of virus genomes and inefficient virus budding was expected to provide a strong evolutionary pressure on the chimeric viruses. This could lead to the selection of rescue mutations with gain of function in virus release. To analyze whether compensatory mutations indeed occur, the chimeric viruses were successively passaged on BSR T7/5 cells. Surprisingly, already after the third passage a substantial gain in virus production and spread in monolayer cell cultures was observed, as indicated by increased virus titers (data not shown) and enlarged foci of infected BSR T7/5 cells 48 h after infection (Fig. 8A). Immediately after rescue, SAD EBLV-1 M produced foci that were 5.5-fold smaller in size than those of SAD RABV M. However, after the third virus passage the foci of SAD EBLV-1Mpass were only 1.6-fold smaller than those of SAD RABV M, indicating that adaptive mutations that support virus spread have occurred in SAD EBLV-1Mpass. In contrast, SAD EBLV-2 M led to similar focus sizes than SAD RABV M, independent of virus passage.

To see whether the increased focus sizes of SAD EBLV-1Mpass correlated with increased infectious virus production, multiple-step growth curves were established of SAD EBLV-1Mpass, SAD EBLV-2Mpass, and SAD RABV M (Fig. 8B). After infection of BSR T7/5 cells at an MOI of 0.01, the cell

Downloaded from jvi.asm.org at FRIEDRICH-LOEFFLER-INSTITUT on February 9, 2010

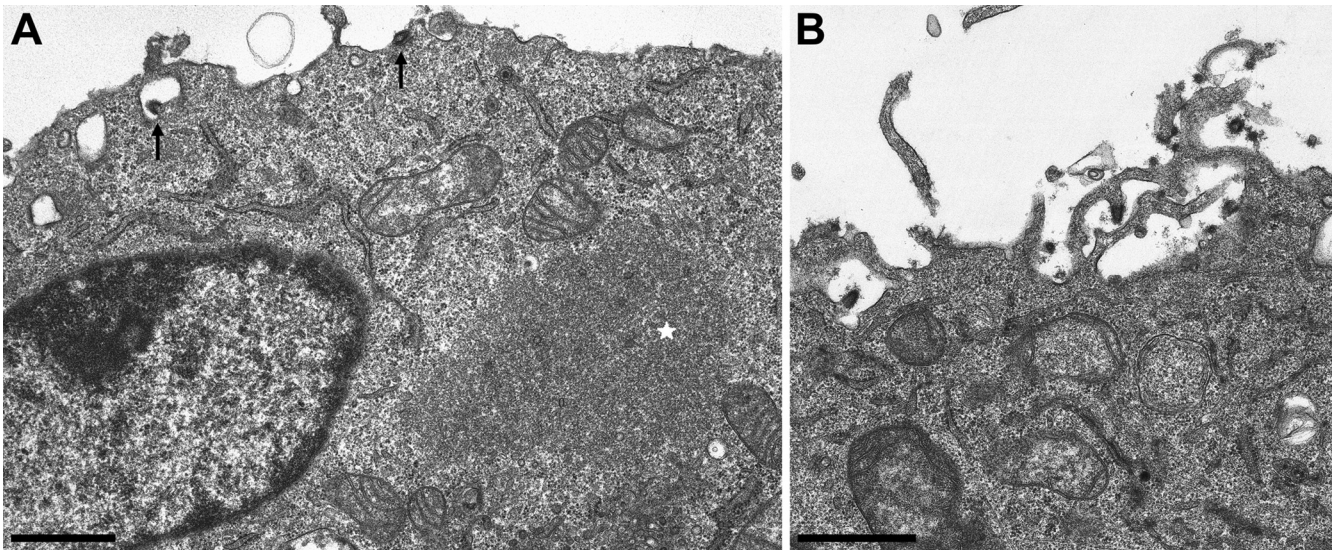

FIG. 6. Intracisternal viruslike structures are not detectable in SAD EBLV-1 M-infected cells. Electron microscopic analysis of SAD EBLV-1 M-infected BSR T7/5 monolayer cell cultures. (A) No intracisternal accumulations of viruslike structures are detectable in SAD EBLV-1 M-infected cells, although RNP inclusion bodies in the cytoplasm (star) and virus budding at the plasma membrane (arrows) indicated virus replication. Scale bar, 1 μm. (B) Virus budding at the plasma membrane (longitudinal section) and after release (cross-section). Scale bar, 1 μm.

culture supernatants were harvested 24, 48, 72, and 96 h p.i., and the infectious virus titers were determined by endpoint dilutions. The results showed that the titers of SAD EBLV-1Mpass and SAD RABV M were comparable, whereas the titers of SAD EBLV-2pass remained five- to sixfold lower.

Intracellular vRNA accumulation is diminished in SAD EBLV-1Mpass-infected cells. With increased infectious virus production by SAD EBLV-1Mpass the intracellular accumulation of virus replication products that was observed for SAD EBLV-1 M (Fig. 3) should decline. To control whether RNA

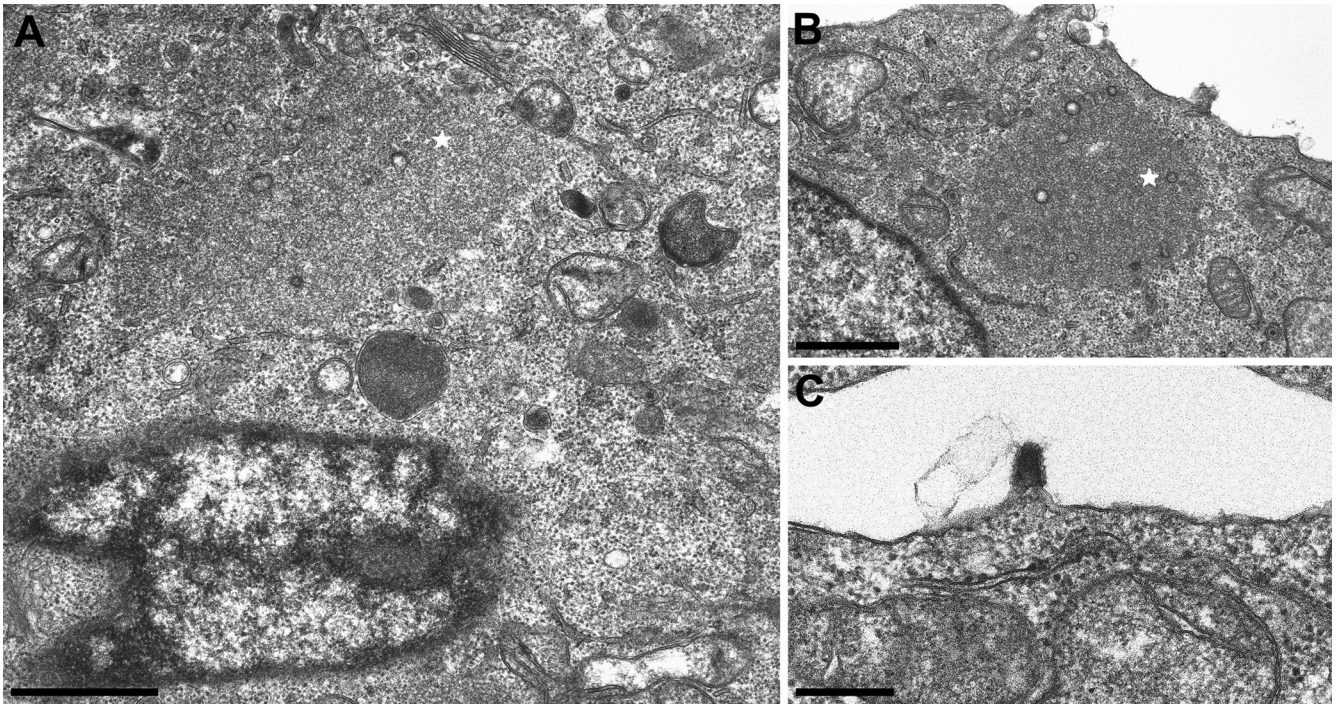

FIG. 7. Intracisternal viruslike structures are not detectable in SAD EBLV-2 M-infected cells. Electron microscopic analysis of SAD EBLV-2 M-infected BSR T7/5 monolayer cell cultures. (A) No intracisternal accumulations of viruslike structures are detectable in SAD EBLV-2 M-infected cells, although RNP inclusion bodies in the cytoplasm (star) indicated virus replication. Scale bar, 1 μm. (B) Cytoplasmic inclusion body (star) and rER without accumulation of intracisternal viruslike structures. Scale bar, 1 μm. (C) Plasma membrane budding of SAD EBLV-2 M. Scale bar, 300 nm.

Downloaded from jvi.asm.org at FRIEDRICH-LOEFFLER-INSTITUT on February 9, 2010

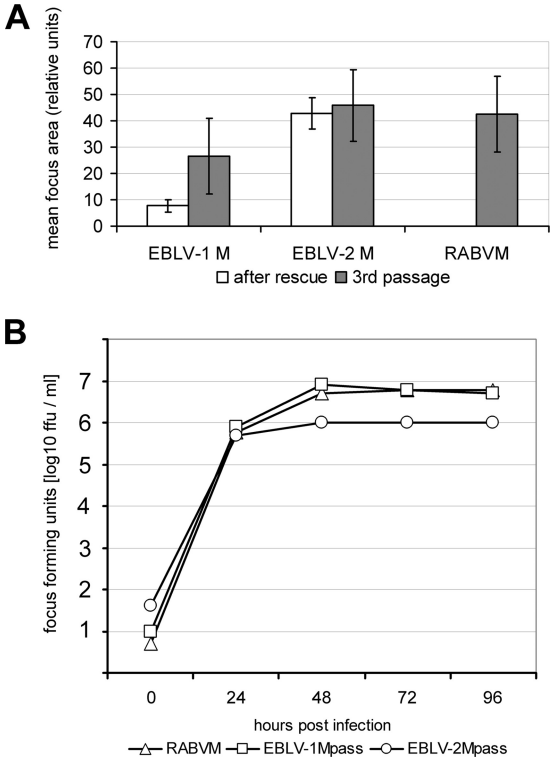

FIG. 8. Selection of chimeric viruses with increased virus release. (A) The ability to spread in cell monolayers was determined for the chimeric viruses directly after virus rescue from cDNAs and after three supernatant passages on BSR T7/5 cell cultures by comparison of the foci of virus-infected cells after 48 h of infection at low MOI. The areas of the foci were measured ($n = 10$). The mean values are provided in the diagram for virus directly after virus rescue (□) and for virus after three supernatant passages (▨). (B) Multiple-step growth kinetics of the passaged chimeras SAD EBLV-1Mpass and SAD EBLV-2Mpass were determined. Whereas SAD EBLV-2Mpass remained five- to six-fold below SAD RABV M, replication of SAD EBLV-1Mpass was comparable to SAD RABV M.

accumulation was altered in SAD EBLV-1Mpass, BSRT7/5 cells were infected with SAD EBLV-1Mpass, SAD EBLV-2Mpass, and SAD RABV M at an MOI of 1. After 2 days RNA was isolated from infected cells and from cell culture supernatant virions after centrifugation through a 20% sucrose cushion. Northern blot hybridizations with an N-gene specific cDNA probe revealed that the levels of full-length vRNA in SAD EBLV1-Mpass-infected cells were lower than in SAD RABV M-infected cells (Fig. 9A, left). For SAD EBLV-1-Mpass only 28% vRNA were detectable (SAD RABV M vRNA = 100%; Fig. 9B, white columns), whereas in SAD EBLV-2Mpass 57% of the SAD RABV M level was achieved. In cell culture supernatants the relative amount of SAD EBLV1-Mpass vRNA increased to 52% of the SAD RABV M level (Fig. 9B, gray columns), whereas for SAD EBLV-2Mpass only 23% extracellular vRNA was detected. These data indicate that mutations in SAD EBLV-1Mpass allowed a more efficient virus release.

Normalization of the N mRNA signal intensities with the detected vRNA signals showed that the mRNA/vRNA ratio in

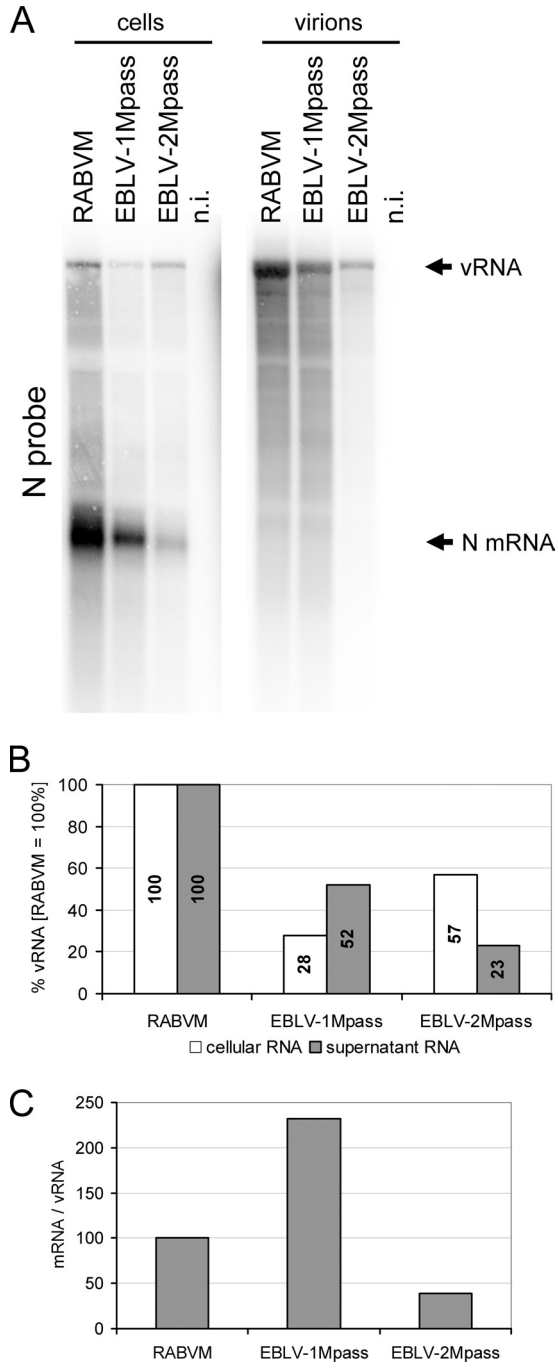

FIG. 9. Northern blot analysis of SAD EBLV-1Mpass and SAD EBLV-2Mpass. RNA was isolated from cells and cell culture supernatants 2 days after infection of BSR T7/5 cells with the indicated viruses. (A) Full-length vRNA and N mRNA were detected with a RABV N gene specific cDNA probe. The signal intensities were quantitated by phosphorimaging. (B) Comparison of vRNA levels in cells (□) and in the supernatant (▨). (C) The ratios of mRNA and vRNA were calculated from signal intensities (SAD RABV M = 100%). Whereas in SAD EBLV-2 M-infected cells the mRNA/vRNA ratio was low, in SAD EBLV-1Mpass-infected cells this ratio increased beyond SAD RABV M, indicating that the accumulation of vRNA observed for SAD EBLV-1 M (see Fig. 3) was lost in SAD EBLV-1Mpass.

Downloaded from jvi.asm.org at FRIEDRICH-LOEFFLER-INSTITUT on February 9, 2010

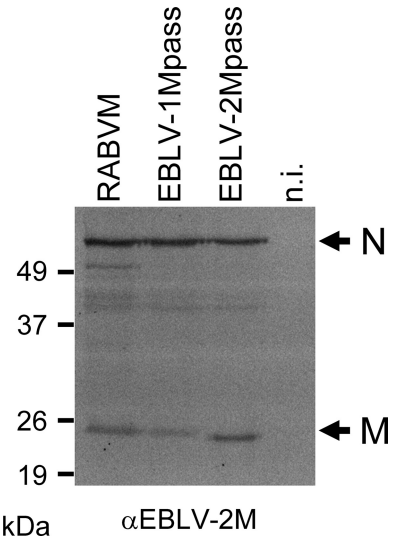

FIG. 10. M protein accumulation in SAD EBLV-1Mpass-infected cells is 2.5-fold decreased compared to SAD RABVM. Cell lysates were prepared from virus-infected cells after 48 h of infection and were analyzed in Western blots with a cross-reactive serum directed against recombinant EBLV-2 M protein. The fluorescent signals were quantitated in a phosphorimager. Since the EBLV-2 M serum recognizes EBLV-1 M protein 1.3-fold better than RABVM protein, a 2.5-decreased M level in SAD EBLV-1Mpass-infected cells was determined. As a second virus protein, RABV N protein was detected with an N-specific serum. Note also that N levels were decreased in SAD EBLV-1Mpass- and SAD EBLV-2Mpass-infected cells.

SAD EBLV-1 M-infected cells was increased compared to SAD RABV M and SAD EBLV-2 M (Fig. 9C).

To determine the viral M gene sequence, the RNA from virus-infected cells (Fig. 9A) was used for RT-PCR amplification and cDNA-sequencing of the complete M ORF of SAD EBLV-1Mpass and SAD EBLV-2Mpass. Whereas in SAD EBLV-2Mpass no mutation was detectable in the M coding region, the EBLV-1Mpass gene exhibited one mutation that led to an amino acid exchange at position 44 from M to K (M44K). Sequencing of the complete N gene and the cytoplasmic domain region of the glycoprotein gene as potential M interacting structures of SAD EBLV-1Mpass did not reveal any further mutation (not shown).

In order to quantitate the level of EBLV-1 M protein relative to RABV M, BSR T7/5 cells were infected as described above and, after 2 days, cell lysates were prepared and analyzed by Western blotting with an EBLV-2 M specific serum that is cross-reactive for all three M proteins expressed. To allow quantification of the Western blot signals, the sensitivity of the serum for the RABV M and EBLV-1 M proteins was determined by normalization of the fluorescent Western blot signals with purified virion-derived M proteins (data not shown). Since the serum recognized EBLV-1 M ~1.3-fold better than RABV M, a 2.5-fold decreased M level was determined for SAD EBLV-1Mpass-infected cells compared to SAD RABV M-infected cells (Fig. 10). The decreased M level correlated with slightly less intensive N protein signals that were detected with a RABV N-protein-specific serum and the observation of decreased virus RNA levels in SAD EBLV-1Mpass-infected cells.

Lack of intracisternal accumulation of viruslike structures in SAD EBLV-1Mpass-infected cells. After selection of efficiently budding SAD EBLV-1Mpass, the accumulation of intracisternal viruslike structures as observed above SAD L16 and SAD RABV M (see Fig. 4 and 5) was investigated. For this purpose, BSR T7/5 cells were infected with SAD EBLV-1Mpass and SAD RABV M at an MOI of 3, and the ultrastructure of the infected cells was analyzed 46 h p.i. As expected, SAD RABV M led to virus assembly by budding at the cell membrane and to the accumulation of viruslike structures in the rER (results not shown). In striking contrast, SAD EBLV-1Mpass exhibited no formation of any viruslike structures at intracytoplasmic membranes (Fig. 11A and B), but virus budding at the plasma membrane occurred (Fig. 11C). The same phenotype was observed in infected Vero cells (data not shown).

These data strongly indicate that the accumulation of viruslike structures in the rER does not correlate with the general assembly and budding activity of the lyssavirus matrix proteins but more likely reflects distinct target membranes of the different M proteins.

DISCUSSION

Among the lyssaviruses conservation of genome organization and a high degree of sequence similarity (11) suggest rather similar mechanisms of virus replication. Nevertheless, different host tropism and pathogenicity among lyssaviruses may indicate the existence of diverse, host-adapted mechanisms of virus replication. A detailed molecular explanation for the distinct behavior of different lyssaviruses is lacking thus far.

One virus protein that has been identified as an important factor of pathogenicity in rabies virus infections is the RABV M protein (12, 39). Whereas previous studies compared attenuated and nonattenuated genotype 1 RABV, in the present study the M proteins of lyssaviruses with different host tropisms were compared to assess the contribution of M to virus replication and virus-host interactions.

In particular, the exchange of the viral M protein between genotype 1 RABV and European bat lyssaviruses EBLV-1 and EBLV-2 and possible impacts on the virus cycle were analyzed by introducing the EBLV M proteins into a genotype 1 virus genetic background. Since M is essential for virus assembly (31, 32), successful intergenotypic complementation was expected to occur only in case of highly conserved interactions during the processes of RNP recruitment and glycoprotein incorporation. Indeed, transcomplementation of NPgrL virus with the M and G genes deleted showed that infectious virus production was 10- and 100-fold decreased after complementation with EBLV-1 M and EBLV-2 M proteins, respectively (see Fig. 1A). These data indicated that the heterologous M proteins were not fully compatible, either in binding to the genotype 1 RNP and/or to the glycoprotein, or with RABV replication.

Whereas EBLV-1 M led to only 10-fold decreased infectious virus titers in the complementation experiments, autonomously replicating chimeric SAD EBLV-1 M was more severely affected in its ability to produce infectious virus than SAD EBLV-2 M. Obviously, in the recombinant virus, EBLV-2 M performed better in complementing RABV M functions than EBLV-1 M, although infectious virus titers after transcomple-

Downloaded from jvi.asm.org at FRIEDRICH-LOEFFLER-INSTITUT on February 9, 2010

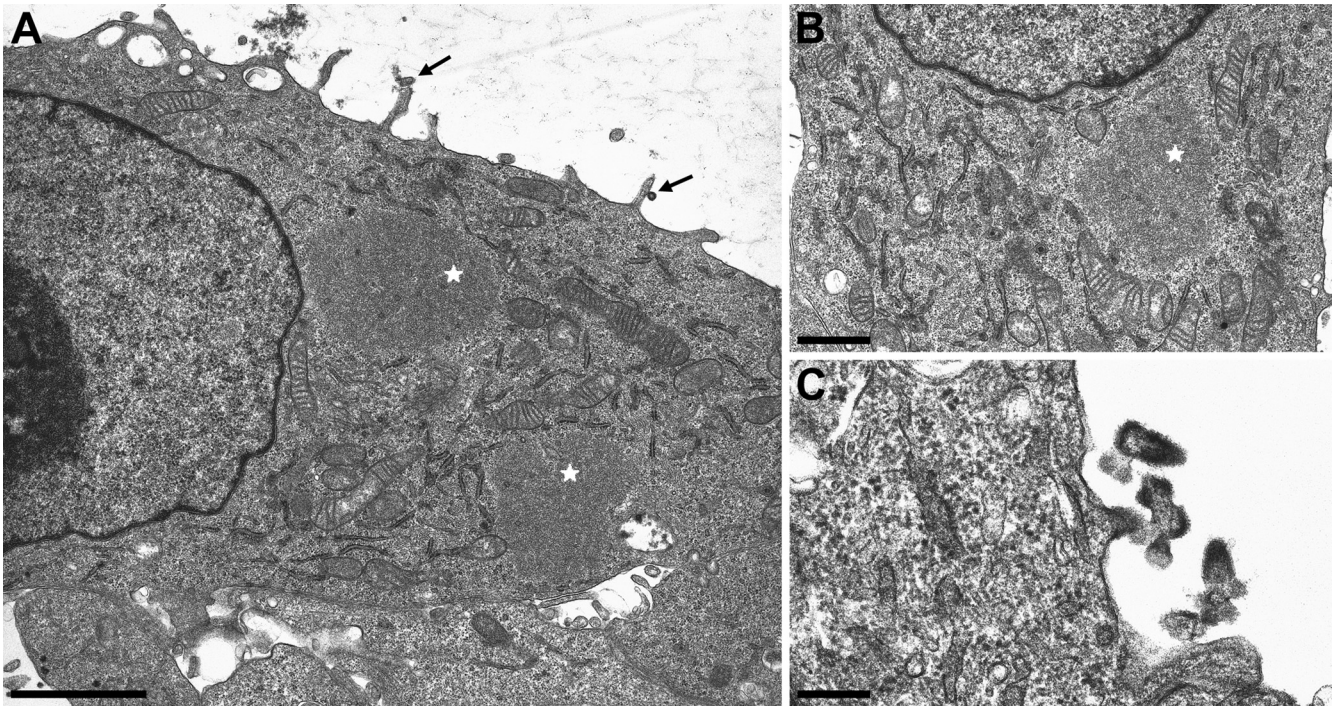

FIG. 11. Increased virus production by SAD EBLV-1Mpass does not result in the formation and accumulation of viruslike structures in the rER. (A) Budding of SAD EBLV-1Mpass at the plasma membrane (arrows) and cytoplasmic inclusion bodies (stars) are shown. No accumulation of viruslike structures in the rER compartment was detectable. The rER appeared to be unaffected. Scale bar, 2 μm. (B) Viral inclusion body (star) and rER without the accumulation of intracisternal viruslike structures. (C) Plasma membrane budding and extracellular bullet shaped virions of SAD EBLV-1Mpass. Scale bar, 250 μm.

mentation were lower than with EBLV-1 M. This discrepancy may be due to the multiple rounds of replication in the full-length clone which can affect both the level of RNA synthesis and virus assembly. In contrast, transcomplementation of minigenome RNPs that accumulated in the absence of M may be rather independent of such non-assembly functions of M. Indeed, previous transcomplementation of minigenomes with different genotype 1 M proteins led only to alterations in the transcript levels, whereas preaccumulated virus genomes remained constant, although complete chimeric RABV with the M proteins integrated in the genome exhibited clearly reduced genome accumulations (14).

Comparable accumulation of vRNA as a replication product in SAD EBLV-1 M- and SAD EBLV-2 M-infected cells (Fig. 3) excluded limiting concentrations of vRNA as the cause for the observed differences in the production of infectious virus. More likely, full-length RNPs accumulated in the infected cells as a consequence of a budding defect. Whereas intracellular accumulation of vRNA could explain reduced infectious virus production, this phenotype was also puzzling since dose-dependent stimulation of replication by M prior to RNP condensation (14, 17) was expected to be less efficient with increasing M sequence divergence. This would result in decreased replication product accumulation. Indeed, with increased infectious virus production in SAD EBLV-1Mpass, the ratio of vRNA and mRNA changed to the opposite, indicating increased transcription in the presence of the heterologous M protein (Fig. 9). Further quantitative studies on mRNA and vRNA levels should shed more light on the regulation of RNA synthesis by the heterogenotypic M.

Intracellular accumulation of RABV RNPs or retention of almost complete virions could be a result of defects in late stages of virus assembly after RNP condensation by M. Indeed, examples for such late domain-defective RABV and other rhabdovirus species have been described (20, 21, 48). Since the late domain PPEY motif in the M proteins of lyssaviruses is conserved, we did not expect a typical late domain-defective phenotype with virus accumulations at the surface of the infected cells. Defects in the assembly pathway could also lead to so-called skeleton-RNPs, which are condensed, M containing nonenveloped subviral structures that are observed after detergent treatment of enveloped VSV and RABV virions (5, 32). Moreover, accumulation of noncondensed RNPs as a result of defects in RNP recruitment by M may occur.

Ultrastructural analyzes revealed that beside budding stages at the cell membrane of all viruses electron dense condensed RNPs inside infected cells were only visible for nonmodified wild-type virus SAD L16 and in SAD RABV M-infected cells, both expressing the RABV M protein. These structures were membrane-enveloped and accumulated in cisternae of the degranulated and dilated rER (see Fig. 4A and B), indicating that budding events have occurred at the rER membrane. Accumulation of intracellular viruslike structures is a common phenomenon in RABV-infected cell cultures and even in primary neurons or neuronal tissues (22, 24, 28, 29, 43). The lack of comparable structures in SAD EBLV-1 M- and SAD EBLV-2

Downloaded from jvi.asm.org at FRIEDRICH-LOEFFLER-INSTITUT on February 9, 2010

M-infected cells, therefore, was surprising, in particular since budding of typical bullet shaped virus particles at the plasma membrane was observed (Fig. 6B and Fig. 7C). Whereas the ability of the heterogenotypic M proteins to support bullet shaped virus particle formation at the plasma membrane showed that these M proteins were basically active in RNP recruitment and membrane envelopment, the decreased virus titers (Fig. 2) strongly indicated that the efficiencies of particle formation were far below those of SAD RABV M.

Although the lack of intracellular budding in SAD EBLV-1 M and SAD EBLV-2 M could be a dose effect in a scenario in which recruitment of RNPs by M is a limiting factor, the efficiently budding SAD EBLV-1Mpass showed that even after increased infectious virus release (Fig. 5C), no intracellular budding events in the rER compartment were detectable. From these data we hypothesize that the RABV and EBLV-1 M proteins target different membranes for virus assembly.

Rapid increase of virus production within only three supernatant passages of SAD EBLV-1 M strongly indicated that adaptive mutations have occurred, either within the EBLV-1 M ORF or in an M interacting protein, making the heterogenotypic EBLV-1 M more compatible to the RABV backbone. Sequencing of SAD EBLV-1 M revealed that a single amino acid exchange at position 44 was evolved during the virus passages. Although no further mutations were detected in the nucleoprotein or in the cytoplasmic domain of the glycoprotein, it remains open whether the M44K mutation indeed contributed to the gain in virus production, and further experiments with regard to the role of the M44K mutation in virus assembly or other M-related functions are needed. Nevertheless, in addition to the detection of the M44K mutation as a thus-far exclusive mutation, the location of the mutation within the three-dimensional structure of lyssavirus M proteins, which was recently determined by Graham et al. (19), is interesting. Although the region around amino acid position 44 was not found in the structure, it is clear that this presumable flexible region separates the globular domain of M from an N-terminal peptide that binds to a hydrophobic pocket within the globular domain during M self-association (Fig. 12). Influences of the M44K mutation on self-association may have contributed to the gain in growth of SAD EBLV-1Mpass. However, based on the structural model, modifications in the interactions of M with the RABV ribonucleoprotein or with other viral structures cannot be excluded.

Similar infectious virus titers in cell culture supernatants of SAD EBLV-1Mpass and SAD RABV M indicated that the intracellular accumulations of viruslike structures do not essentially contribute to the release of infectious virus, raising the question about their biological function. As shown by cross-sections of wild-type SAD L16 virions and intracellular viruslike structures in the degranulated rER, diameters and inner ultrastructure of the virus bodies were identical with extracellular virions (Fig. 4B and C), indicating that indeed membrane-enveloped, condensed RNPs were formed by budding into the rER lumen. Since RABV M is essential for RNP condensation (32), these structures should contain all inner structural components of a virion. However, as evident from previous observations (22), longitudinal sections demonstrated that the RNP structures were more variable in length than those that are typically observed in extracellular virions.

```
RABV    MNLLRKIVKNRRDEDTQKSSPASAPLDDDDLWLPPPEYVP 40
EBLV-2  --f----rgc---ed--palv---p---------------- 40
EBLV-1  --ii----sck-dem--pn-v---p---------------- 40

RABV    LKELTGKKNMRNFCINGRVKVCSPNGYSFRILRHILKSFD 80
EBLV-2  -t-i--r-------v--e-------------------r--- 80
EBLV-1  -s-m--r----------e-----------i----s--e 80

RABV    EIYSGNHRMIGLVKVVIGLALSGSPVPEGLNWVYKLRRTF 120
EBLV-2  gv----q--r----------d---g-i---m-----v---l 120
EBLV-1  gv----r----------------a---d-m-----i---l 120

RABV    IFQWADSRGPLEGEELEYSQEITWDDDTEFVGLQIRVIAK 160
EBLV-2  v----e-----d----------------s---------s-r 160
EBLV-1  -----e-s---d----------------s------m--s-r 160

RABV    QCHIQGRVWCINMNPRACQLWSDMSLQTQRSEEDKDSSLL 200
EBLV-2  -------i------s---------a-k--q-d--rnt--- 200
EBLV-1  -------l------s----------k--q-d---nt--- 200

RABV    LE                                        202
EBLV-2  --                                        202
EBLV-1  --                                        202
```

FIG. 12. Amino acid sequence comparison of the lyssavirus M proteins that were introduced into the recombinant viruses SAD RABVM, SAD EBLV-1 M, and SAD EBLV-2 M. Amino acids in EBLV-1 M and EBLV-2 M that diverged from RABV M are indicated by lowercase letters. Positively charged amino acids within the N-terminal region are highlighted in blue. Amino acids that are involved in M self-association are highlighted in gray. A short region that is not detected in the structure of Lagos bat virus M is marked by a red box. A methionine residue in EBLV-1 M, which was mutated in EBLV-1Mpass, is highlighted in red.

Whereas the intracellular viruslike structures most likely did not contribute to infectivity in cell cultures, a role in neurotropism and disease development cannot be ruled out. The observed accumulations of viruslike particles are commonly observed for the neurotropic lyssaviruses, and only few examples of nonlyssavirus rhabdoviruses with comparable accumulations exist. One example is the neurotropic Oita rhabdovirus that combines several characteristics of lyssa- and vesiculoviruses and was shown to produce enveloped viruslike structures in the ER (23). Although no experimental data corroborate previous speculations about the role of the intracellular assembly structures in intraneuronal RNP transport (43), this hypothesis is attractive in terms of intraneuronal long-distance transport of newly synthesized RNPs or viruslike structures without the need of budding to the extracellular space. This would also explain why in standard cell cultures the intracellular RNP accumulations do not contribute to the production of infectious virus.

Intracellular accumulations could also simply occur by budding at the ER membrane as a result of excess RABV M and G proteins in late stages of infection. M-RNP complexes at high intracellular concentrations could interact with ER membranes, and subsequent budding may occur. However, the lack of intracellular accumulations in SADEBLV-1Mpass-infected cells argues against a simple overproduction and unspecific budding at the rER membrane. SAD EBLV-1Mpass, which replicated efficiently, as demonstrated by growth curves identical to SAD RABV M (Fig. 8B), was efficiently replicating and infectious virus production was comparable to SAD RABV M, although the levels of intracellular viral RNAs (Fig. 9A) and protein levels (Fig. 10) were slightly decreased. Whereas this

Downloaded from jvi.asm.org at FRIEDRICH-LOEFFLER-INSTITUT on February 9, 2010

could hint on a dose-dependent accumulation of intracellular viruslike structures, it is unlikely that the only 2.5-fold-decreased M protein level was causative for the complete lack of intracellular viruslike structures. Overproduction of M and G would also be expected at least in part of the SAD EBLV-1Mpass-infected cells. The complete lack of the intracellular assembly structures strongly indicates that the EBLV-1 M protein differs in its specificity either to cellular membranes or to membrane-associated proteins that are involved in virus budding.

Membrane binding by lyssavirus M proteins has not yet been addressed adequately thus far. Because positively charged amino acids are located in the N-terminal region of the lyssavirus M proteins, membrane binding is thought to occur similarly to vesicular stomatitis virus (VSV) M. For VSV M, it has been shown that the N terminus is required for membrane binding and, in addition, a second membrane-binding region in the globular domain of VSV M has been described (10). Interestingly, amino acids within this second membrane binding region are also involved in binding of N-terminal residues during the process of self-association, which has been suggested to enhance membrane binding of both, VSV M and lyssavirus M proteins (19). Since both positively charged N-terminal residues and those residues that are involved in M self-association are highly conserved (see Fig. 12), it appears unlike that these motifs contribute to the different phenotypes of the EBLV-1 M and RABV M proteins in the assembly of intracellular viruslike structures. Thus, membrane specificity in lyssavirus budding may be determined by other regions or motifs within the lyssavirus M proteins.

Indeed, preliminary experiments with EBLV-1 also indicate a lack of intracellular viruslike structures (results not shown). A direct comparison to the results shown here, however, is difficult because of the lower replication levels of EBLV-1 compared to RABV. In particular, in view of low pathogenicity in experimental EBLV-1 infections of terrestrial mammals (1), further experiments are required to assess whether the ability to form viruslike structures in the rER compartment correlates with the degree of neurovirulence or virus transmission.

With the intergenotypic comparison of M functions on an identical genetic background, we provide for the first time strong evidence that the matrix proteins of lyssaviruses exhibit diverse and genotype specific functions in the process of virus assembly. This may result in the use of different membranes for virus assembly. On the other hand, basal intraviral interactions that are required for virus assembly and release appear rather conserved, as indicated by the general possibility of intergenotypic complementation and fast selection of efficiently replicating SAD EBLV-1Mpass. A detailed analysis of SAD EBLV-1Mpass shall uncover the role of the M44K mutation within the M gene or other virus proteins that are important for lyssavirus assembly and release. This may also provide a new basis for the identification of virus protein interactions that regulate RNP condensation and particle assembly.

ACKNOWLEDGMENTS

We are grateful to Karl Klaus Conzelmann (Max von Pettenkofer Institute, Munich, Germany) for providing of the RABV full-length cDNA clone pSAD L16. We thank Dietlind Kretzschmar, Angela Hillner, Mandy Jörn, and Petra Mayer for technical assistance and Thomas Müller (Friedrich-Loeffler-Institut, Wusterhausen, Germany) for helpful discussions and critical comments on the manuscript.

This study was supported by the Deutsche Forschungsgemeinschaft through DFG FI941/3-1 and DFG FI941/4-2.

REFERENCES

1. **Brookes, S. M., R. Klopfleisch, T. Muller, D. M. Healy, J. P. Teifke, E. Lange, J. Kliemt, N. Johnson, L. Johnson, V. Kaden, A. Vos, and A. R. Fooks.** 2007. Susceptibility of sheep to European bat lyssavirus type-1 and -2 infection: a clinical pathogenesis study. Vet. Microbiol. **125:**210–223.
2. **Brzozka, K., S. Finke, and K. K. Conzelmann.** 2005. Identification of the rabies virus alpha/beta interferon antagonist: phosphoprotein P interferes with phosphorylation of interferon regulatory factor 3. J. Virol. **79:**7673–7681.
3. **Brzozka, K., S. Finke, and K. K. Conzelmann.** 2006. Inhibition of interferon signaling by rabies virus phosphoprotein P: activation-dependent binding of STAT1 and STAT2. J. Virol. **80:**2675–2683.
4. **Buchholz, U. J., S. Finke, and K. K. Conzelmann.** 1999. Generation of bovine respiratory syncytial virus (BRSV) from cDNA: BRSV NS2 is not essential for virus replication in tissue culture, and the human RSV leader region acts as a functional BRSV genome promoter. J. Virol. **73:**251–259.
5. **Cartwright, B., C. J. Smale, and F. Brown.** 1970. Dissection of vesicular stomatitis virus into the infective ribonucleoprotein and immunizing components. J. Gen. Virol. **7:**19–32.
6. **Chelbi-Alix, M. K., A. Vidy, B. J. El, and D. Blondel.** 2006. Rabies viral mechanisms to escape the IFN system: the viral protein P interferes with IRF-3, Stat1, and PML nuclear bodies. J. Interferon Cytokine Res. **26:**271–280.
7. **Cliquet, F., E. Picard-Meyer, J. Barrat, S. M. Brookes, D. M. Healy, M. Wasniewski, E. Litaize, M. Biarnais, L. Johnson, and A. R. Fooks.** 2009. Experimental infection of foxes with European bat lyssaviruses types 1 and 2. BMC. Vet. Res. **5:**19.
8. **Conzelmann, K. K., and M. Schnell.** 1994. Rescue of synthetic genomic RNA analogs of rabies virus by plasmid-encoded proteins. J. Virol. **68:**713–719.
9. **Dacheux, L., F. Larrous, A. Mailles, D. Boisseleau, O. Delmas, C. Biron, C. Bouchier, I. Capek, M. Muller, F. Ilari, T. Lefranc, F. Raffi, M. Goudal, and H. Bourhy.** 2009. Lyssavirus transmission among cats, Europe. Emerg. Infect. Dis. **15:**280–284.
10. **Dancho, B., M. O. McKenzie, J. H. Connor, and D. S. Lyles.** 2009. Vesicular stomatitis virus matrix protein mutations that affect association with host membranes and viral nucleocapsids. J. Biol. Chem. **284:**4500–4509.
11. **Delmas, O., E. C. Holmes, C. Talbi, F. Larrous, L. Dacheux, C. Bouchier, and H. Bourhy.** 2008. Genomic diversity and evolution of the lyssaviruses. PLoS. One **3:**e2057.
12. **Faber, M., R. Pulmanausahakul, K. Nagao, M. Prosniak, A. B. Rice, H. Koprowski, M. J. Schnell, and B. Dietzschold.** 2004. Identification of viral genomic elements responsible for rabies virus neuroinvasiveness. Proc. Natl. Acad. Sci. U. S. A. **101:**16328–16332.
13. **Fauquet, C. M., M. A. Mayo, J. Maniloff, U. Desselberger, and L. A. Ball (ed.).** 2005. Virus taxonomy: VIIIth report of the International Committee on Taxonomy and Viruses. Elsevier/Academic Press, London, England.
14. **Finke, S., and K. K. Conzelmann.** 2003. Dissociation of rabies virus matrix protein functions in regulation of viral RNA synthesis and virus assembly. J. Virol. **77:**12074–12082.
15. **Finke, S., and K. K. Conzelmann.** 2005. Replication strategies of rabies virus. Virus Res. **111:**120–131.
16. **Finke, S., and K. K. Conzelmann.** 1999. Virus promoters determine interference by defective RNAs: selective amplification of mini-RNA vectors and rescue from cDNA by a 3′ copy-back ambisense rabies virus. J. Virol. **73:**3818–3825.
17. **Finke, S., R. Mueller-Waldeck, and K. K. Conzelmann.** 2003. Rabies virus matrix protein regulates the balance of virus transcription and replication. J. Gen. Virol. **84:**1613–1621.
18. **Gholami, A., R. Kassis, E. Real, O. Delmas, S. Guadagnini, F. Larrous, D. Obach, M. C. Prevost, Y. Jacob, and H. Bourhy.** 2008. Mitochondrial dysfunction in lyssavirus-induced apoptosis. J. Virol. **82:**4774–4784.
19. **Graham, S. C., R. Assenberg, O. Delmas, A. Verma, A. Gholami, C. Talbi, R. J. Owens, D. I. Stuart, J. M. Grimes, and H. Bourhy.** 2008. Rhabdovirus matrix protein structures reveal a novel mode of self-association. PLoS Pathog. **4:**e1000251.
20. **Harty, R. N., M. E. Brown, J. P. McGettigan, G. Wang, H. R. Jayakar, J. M. Huibregtse, M. A. Whitt, and M. J. Schnell.** 2001. Rhabdoviruses and the cellular ubiquitin-proteasome system: a budding interaction. J. Virol. **75:**10623–10629.
21. **Harty, R. N., J. Paragas, M. Sudol, and P. Palese.** 1999. A proline-rich motif within the matrix protein of vesicular stomatitis virus and rabies virus interacts with WW domains of cellular proteins: implications for viral budding. J. Virol. **73:**2921–2929.
22. **Hummeler, K., H. Koprowski, and T. J. Wiktor.** 1967. Structure and development of rabies virus in tissue culture. J. Virol. **1:**152–170.

Downloaded from jvi.asm.org at FRIEDRICH-LOEFFLER-INSTITUT on February 9, 2010

23. **Iwasaki, T., S. Inoue, K. Tanaka, Y. Sato, S. Morikawa, D. Hayasaka, M. Moriyama, T. Ono, S. Kanai, A. Yamada, and T. Kurata.** 2004. Characterization of Oita virus 296/1972 of *Rhabdoviridae* isolated from a horseshoe bat bearing characteristics of both lyssavirus and vesiculovirus. Arch. Virol. **149:** 1139–1154.
24. **Iwasaki, Y., S. Ohtani, and H. F. Clark.** 1975. Maturation of rabies virus by budding from neuronal cell membrane in suckling mouse brain. J. Virol. **15:**1020–1023.
25. **Kassis, R., F. Larrous, J. Estaquier, and H. Bourhy.** 2004. Lyssavirus matrix protein induces apoptosis by a TRAIL-dependent mechanism involving caspase-8 activation. J. Virol. **78:**6543–6555.
26. **Le, M. P., Y. Jacob, K. Tanner, and N. Tordo.** 2002. A novel expression cassette of lyssavirus shows that the distantly related Mokola virus can rescue a defective rabies virus genome. J. Virol. **76:**2024–2027.
27. **Marston, D. A., L. M. McElhinney, N. Johnson, T. Muller, K. K. Conzelmann, N. Tordo, and A. R. Fooks.** 2007. Comparative analysis of the full genome sequence of European bat lyssavirus type 1 and type 2 with other lyssaviruses and evidence for a conserved transcription termination and polyadenylation motif in the G-L 3′ non-translated region. J. Gen. Virol. **88:**1302–1314.
28. **Matsumoto, S.** 1963. Electron microscope studies of rabies virus in mouse brain. J. Cell Biol. **19:**565–591.
29. **Matsumoto, S., L. G. Schneider, A. Kawai, and T. Yonezawa.** 1974. Further studies on the replication of rabies and rabies-like viruses in organized cultures of mammalian neural tissues. J. Virol. **14:**981–996.
30. **Mebatsion, T.** 2001. Extensive attenuation of rabies virus by simultaneously modifying the dynein light chain binding site in the P protein and replacing Arg333 in the G protein. J. Virol. **75:**11496–11502.
31. **Mebatsion, T., M. Konig, and K. K. Conzelmann.** 1996. Budding of rabies virus particles in the absence of the spike glycoprotein. Cell **84:**941–951.
32. **Mebatsion, T., F. Weiland, and K. K. Conzelmann.** 1999. Matrix protein of rabies virus is responsible for the assembly and budding of bullet-shaped particles and interacts with the transmembrane spike glycoprotein G. J. Virol. **73:**242–250.
33. **Morimoto, K., H. D. Foley, J. P. McGettigan, M. J. Schnell, and B. Dietzschold.** 2000. Reinvestigation of the role of the rabies virus glycoprotein in viral pathogenesis using a reverse genetics approach. J. Neurovirol. **6:**373–381.
34. **Morimoto, K., D. C. Hooper, S. Spitsin, H. Koprowski, and B. Dietzschold.** 1999. Pathogenicity of different rabies virus variants inversely correlates with apoptosis and rabies virus glycoprotein expression in infected primary neuron cultures. J. Virol. **73:**510–518.
35. **Muller, T., J. Cox, W. Peter, R. Schafer, N. Johnson, L. M. McElhinney, J. L. Geue, K. Tjornehoj, and A. R. Fooks.** 2004. Spill-over of European bat lyssavirus type 1 into a stone marten (Martes foina) in Germany. J. Vet. Med. B Infect. Dis. Vet. Public Health **51:**49–54.
36. **Murphy, F. A., S. P. Bauer, A. K. Harrison, and W. C. Winn, Jr.** 1973. Comparative pathogenesis of rabies and rabies-like viruses. Viral infection and transit from inoculation site to the central nervous system. Lab. Invest. **28:**361–376.
37. **Murphy, F. A., A. K. Harrison, W. C. Winn, and S. P. Bauer.** 1973. Comparative pathogenesis of rabies and rabies-like viruses: infection of the central nervous system and centrifugal spread of virus to peripheral tissues. Lab. Invest. **29:**1–16.
38. **Niwa, H., K. Yamamura, and J. Miyazaki.** 1991. Efficient selection for high-expression transfectants with a novel eukaryotic vector. Gene **108:**193–199.
39. **Pulmanausahakul, R., J. Li, M. J. Schnell, and B. Dietzschold.** 2008. The glycoprotein and the matrix protein of rabies virus affect pathogenicity by regulating viral replication and facilitating cell-to-cell spread. J. Virol. **82:** 2330–2338.
40. **Schnell, M. J., T. Mebatsion, and K. K. Conzelmann.** 1994. Infectious rabies viruses from cloned cDNA. EMBO J. **13:**4195–4203.
41. **Tan, G. S., M. A. Preuss, J. C. Williams, and M. J. Schnell.** 2007. The dynein light chain 8 binding motif of rabies virus phosphoprotein promotes efficient viral transcription. Proc. Natl. Acad. Sci. U. S. A. **104:**7229–7234.
42. **Tjornehoj, K., A. R. Fooks, J. S. Agerholm, and L. Ronsholt.** 2006. Natural and experimental infection of sheep with European bat lyssavirus type-1 of Danish bat origin. J. Comp. Pathol. **134:**190–201.
43. **Velandia, M. L., R. Perez-Castro, H. Hurtado, and J. E. Castellanos.** 2007. Ultrastructural description of rabies virus infection in cultured sensory neurons. Mem. Inst. Oswaldo Cruz **102:**441–447.
44. **Vidy, A., M. Chelbi-Alix, and D. Blondel.** 2005. Rabies virus P protein interacts with STAT1 and inhibits interferon signal transduction pathways. J. Virol. **79:**14411–14420.
45. **Vidy, A., B. J. El, M. K. Chelbi-Alix, and D. Blondel.** 2007. The nucleocytoplasmic rabies virus P protein counteracts interferon signaling by inhibiting both nuclear accumulation and DNA binding of STAT1. J. Virol. **81:**4255–4263.
46. **Vos, A., T. Muller, J. Cox, L. Neubert, and A. R. Fooks.** 2004. Susceptibility of ferrets (*Mustela putorius furo*) to experimentally induced rabies with European bat lyssaviruses (EBLV). J. Vet. Med. B Infect. Dis. Vet. Public Health **51:**55–60.
47. **Vos, A., T. Muller, L. Neubert, A. Zurbriggen, C. Botteron, D. Pohle, H. Schoon, L. Haas, and A. C. Jackson.** 2004. Rabies in red foxes (*Vulpes vulpes*) experimentally infected with European bat lyssavirus type 1. J. Vet. Med. B Infect. Dis. Vet. Public Health **51:**327–332.
48. **Wirblich, C., G. S. Tan, A. Papaneri, P. J. Godlewski, J. M. Orenstein, R. N. Harty, and M. J. Schnell.** 2008. PPEY motif within the rabies virus (RV) matrix protein is essential for efficient virion release and RV pathogenicity. J. Virol. **82:**9730–9738.

Downloaded from jvi.asm.org at FRIEDRICH-LOEFFLER-INSTITUT on February 9, 2010